Available online at www.sciencedirect.com
ScienceDirect
Trans. Nonferrous Met. Soc. China 29(2019) 650−656

Transactions of Nonferrous Metals Society of China
www.tnmsc.cn

Effect of P addition on mineral transition of $CaO-Al_2O_3-SiO_2$ system during high-temperature sintering

Hai-yan YU, Xiao-lin PAN, Kai-wei DONG, Yan WU

School of Metallurgy, Northeastern University, Shenyang 110819, China

Received 8 March 2018; accepted 12 June 2018

Abstract: The mineral transition, microstructure and self-pulverization as well as the Al_2O_3 leaching performance of calcium aluminate clinkers with different P additions in $CaO-Al_2O_3-SiO_2$ system during high-temperature sintering were systematically studied by XRF, XRD, SEM−EDS and DSC−TG technologies. The clinkers sintered at 1350 °C mainly contain $12CaO\cdot7Al_2O_3$, $CaO\cdot Al_2O_3$, β-$2CaO\cdot SiO_2$ and γ-$2CaO\cdot SiO_2$. The content of β-$2CaO\cdot SiO_2$ increases while the content of γ-$2CaO\cdot SiO_2$ decreases as the P addition increases. The self-pulverization property of clinkers deteriorates with increasing P addition. P distributes evenly in the clinkers, and inhibits the transformation of β-$2CaO\cdot SiO_2$ to γ-$2CaO\cdot SiO_2$. The cell volumes of $12CaO\cdot7Al_2O_3$ and $CaO\cdot Al_2O_3$ decrease and increase respectively as the P addition increases, and P decreases their formation temperatures. The Al_2O_3 leaching rate of calcium aluminate clinkers decreases obviously with increasing P addition, which decreases form 95.01% to 83.84% as the P addition increases from 0 to 0.85%.

Key words: lime-sinter process; calcium aluminate; dicalcium silicate; crystal structure; self-pulverization performance; leaching

---

1 Introduction

Calcium aluminate compounds in $CaO-Al_2O_3-SiO_2$ ternary system are the research focus in basic theories and applications, which have played an important role in the areas of refractories, oxide ceramics, cement chemistry, metallurgical slags and geochemistry [1−4]. The calcium aluminates are mainly comprised of $3CaO\cdot Al_2O_3$ (C_3A), $12CaO\cdot7Al_2O_3$ ($C_{12}A_7$), $CaO\cdot Al_2O_3$ (CA), $CaO\cdot2Al_2O_3$ (CA_2), $CaO\cdot6Al_2O_3$ (CA_6) [5]. Combustion synthesis and mechanical activation were used to synthesize calcium aluminates by RODRÍGUEZ et al [6] and CHEN [7]; MOHAMED and SHARP [8,9] obtained the formation mechanism and microstructure characteristics of CA and C_3A; OSTROWSKI and ELAZNY [10] determined the solid solutions of calcium aluminates; STÖBER et al [11] and VERMA et al [12] studied the crystal structure and physical-chemical properties in Mn^{4+}, Mn^{2+}, Fe^{3+} and Tb^{3+} doped $C_{12}A_7$ and other aluminates, respectively.

Calcium aluminates are also the main constitutes of sintering clinker in the lime-sinter process from alumina industry [13]. TIAN et al [14] and ZHANG et al [15] studied the formation mechanisms of different calcium aluminate compounds with different molar ratios of CaO to Al_2O_3 in $CaO-Al_2O_3$ system and $CaO-Al_2O_3-SiO_2$ system respectively, and found that the calcium aluminates present as a layered distribution and all the calcium aluminates play role as the intermediate phases to the final equilibrium phases. YU et al [16,17] discussed the effects of Na_2O and iron oxides on the formation activity of calcium aluminate clinker, and found that Na_2O and FeO can form solid solutions in $C_{12}A_7$ and inhibit the transformation of β-$2CaO\cdot SiO_2$ to γ-$2CaO\cdot SiO_2$. WANG et al [18,19] investigated the effects of MgO and S on the mineral transition and leaching properties of calcium aluminate clinkers, and found that they can form $20CaO\cdot13Al_2O_3\cdot3MgO\cdot3SiO_2$ and $3CaO\cdot3Al_2O_3\cdot CaSO_4$, respectively. However, as an important impurity in bauxite ores and other raw materials, the effects of P on the formation process and leaching properties of calcium aluminate clinkers are unknown. The content of P in bauxites usually ranges from 0.05% to 0.5% in the mineral form of apatite. In this work, the self-pulverization, sintering characteristics and leaching properties of calcium aluminate clinkers with different P additions were systematically investigated

---

Foundation item: Projects (51674075, 51774079) supported by the National Natural Science Foundation of China

Corresponding author: Xiao-lin PAN; Tel: +86-24-83686460; E-mail: panxl@smm.neu.edu.cn

DOI: 10.1016/S1003-6326(19)64975-7

in the $CaO-Al_2O_3-SiO_2$ system based on the lime-sinter process.

2 Experimental

Analytically pure reagents of $CaCO_3$, Al_2O_3, SiO_2 and $Ca_3(PO_4)_2$ were used in this study, and the calculated mass fractions of oxides for the sintering process are 49.70% CaO, 10.06% SiO_2, 40.24% Al_2O_3 and 0−0.85% P. Then, the mixtures were milled in a ball mill for 3 h. A programmable $MoSi_2$ heating furnace was used for sintering in a graphite crucible at 1350 °C for 1 h, and then the clinkers were cooled to room temperature in the furnace after sintering.

The calcium aluminate clinkers were ground to below 74 μm in particle size and then leached at 80 °C for 30 min in sodium carbonate solution. The concentration of sodium carbonate solution (in form of Na_2O) is 80 g/L. The liquid-to-solid ratio of sodium carbonate solution to clinker for leaching is 10:1. The leached slurry was filtrated using a Buchner funnel. The concentrations of caustic alkali (N_K, in form of Na_2O), total alkali (N_T, in form of Na_2O) and Al_2O_3 (AO) in the filtrate were determined by the volumetric method, and the filter residues were washed with hot water and dried for chemical analysis. The Al_2O_3 leaching rate ($\eta_{Al_2O_3}$) is calculated according to the following formula:

$$\eta_{Al_2O_3}=\frac{(m_A/m_S)_{clinker}-(m_A/m_S)_{residue}}{(m_A/m_S)_{clinker}}\times 100\% \tag{1}$$

where $(m_A/m_S)_{clinker}$ and $(m_A/m_S)_{residue}$ are the mass ratios of Al_2O_3 to SiO_2 in the sintered clinkers and leached residues, respectively.

The contents of Al_2O_3 and SiO_2 in the sintered clinkers and leached residues were determined using X-ray fluorescence (XRF, ZSX100e) [20]. The mineral compositions of clinkers and residues were estimated by X-ray diffraction (PANalytical PW3040/60). Quantitative analyses were performed by the Rietveld refinement method. The differential scanning calorimetry (DSC) and thermogravimetric (TG) analysis were performed using NETZSCH STA409C/CD simultaneous thermal analyzer in dynamic Ar atmosphere with a heating rate of 10 °C/min. The morphology and micro-composition of minerals in clinker were obtained by SEM (SHIMADZU SSX−550) coupled with EDS (DX−4).

3 Results and discussion

3.1 Pulverization property of calcium aluminate clinkers

The macrostructures of calcium aluminate clinkers with different P additions are shown in Fig. 1. The clinker without P is pulverized very well; as the P addition increases to 0.50%, about 40% of the clinker is not pulverized as vitreous particles, which is over 74 μm in particle size, and the other is shown in Fig. 1(b); when the P addition is 0.85%, the clinker is absolutely not pulverized.

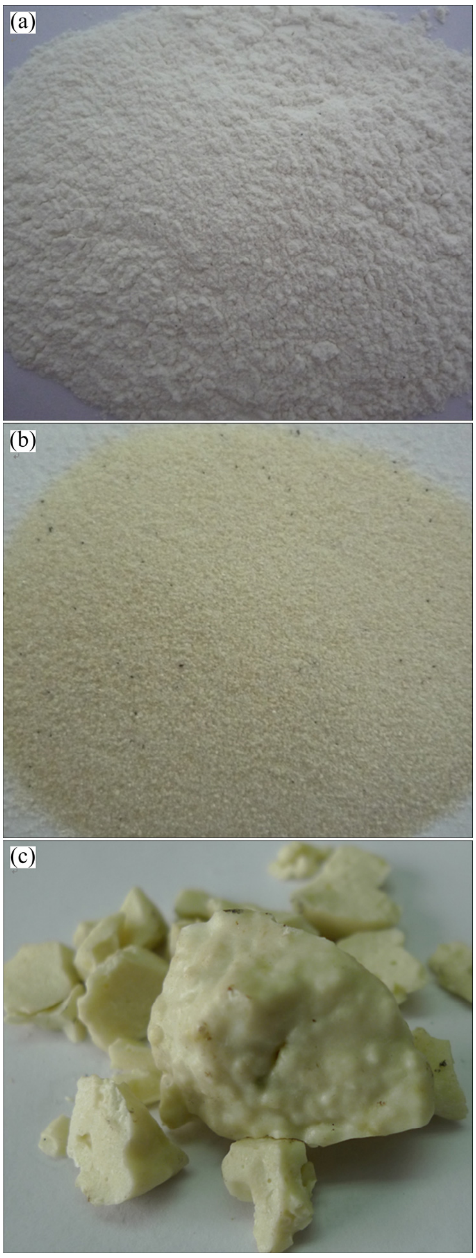

Fig. 1 Macrostructures of calcium aluminate clinkers with different P additions: (a) Without P; (b) 0.50% P; (c) 0.85% P

The main sintering reactions of $CaO-Al_2O_3-SiO_2$ ternary system at 1350 °C are the formation of calcium aluminates and dicalcium silicate, as shown in Formulae (2) and (3). Dicalcium silicate ($2CaO\cdot SiO_2$, C_2S) has a variety of crystal structures [21], e.g. α, α'_H, α'_L, β and γ, which transform to each other under different conditions. The crystal of C_2S during the lime-sinter process transforms from β to γ at (700±20) °C during the cooling process of calcium aluminate clinkers. The volume of clinkers will expand about 10% during the transformation process because of different relative densities of the two types of C_2S (the densities of β-C_2S and γ-C_2S are 3.28 and 2.97 g/cm^3, respectively). Then, the internal stress in the inner crystals of C_2S will make the clinker pulverized itself. The pulverization properties of calcium aluminate clinkers get much worse with increasing P addition, as shown in Fig. 1, indicating that P inhibits the transformation of β-2C_2S to γ-2C_2S. The reason may be that P can enter into the crystal lattice of C_2S and forms solid solutions, and then the glassy structure will form in the cooling process, as seen in Fig. 1(c), which inhibits the β to γ transformation. In fact, B_2O_3, Na_2O, K_2O, MgO, BaO, MnO_2 and Cr_2O_3 were also reported to stabilize β-C_2S [22].

$$m\text{CaO(s)}+n\text{Al}_2\text{O}_3\text{(s)}\longrightarrow m\text{CaO}\cdot n\text{Al}_2\text{O}_3\text{(s)} \qquad (2)$$

$$2\text{CaO(s)}+\text{SiO}_2\text{(s)}\longrightarrow 2\text{CaO}\cdot\text{SiO}_2\text{(s)} \qquad (3)$$

3.2 Mineral transition of calcium aluminate clinkers

The XRD patterns of calcium aluminate clinkers with different P additions are shown in Fig. 2. All the clinkers contain $C_{12}A_7$, CA, β-C_2S and γ-C_2S, and the P impurity does not affect the phase types of calcium aluminate clinkers. However, the mineral contents in clinkers are different. The peak intensity of γ-C_2S decreases and the peak intensity of β-C_2S increases as the P addition increases, as seen in Fig. 2.

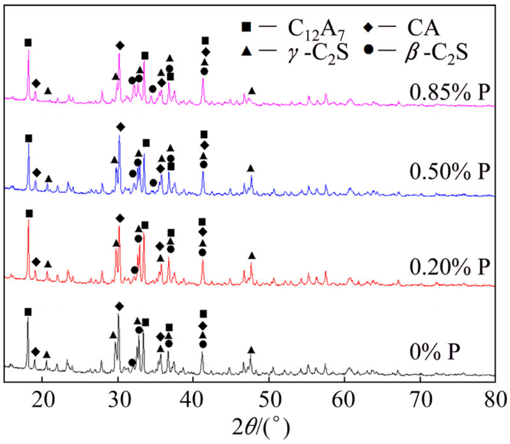

Fig. 2 XRD patterns of calcium aluminate clinkers with different P additions

The mineral compositions in calcium aluminate clinkers with different P additions were calculated by the Rietveld method as listed in Table 1. The contents of $C_{12}A_7$ and CA do not change obviously, but the contents of β-C_2S and γ-C_2S change accordingly with increasing P addition. When there is no P addition, C_2S is mainly in the form of γ-C_2S. However, as the P addition increases, the content of γ-C_2S decreases while the content of β-C_2S increases. When the P addition is 0.85%, β-C_2S is the dominant existence of C_2S. The above results are consistent with the self-pulverization properties of calcium aluminate clinkers, which demonstrate that the P impurity restrains the transformation of β-C_2S to γ-C_2S.

Table 1 Mineral compositions in calcium aluminate clinkers with different P additions (wt.%)

P addition/wt.%	$C_{12}A_7$	CA	γ-C_2S	β-C_2S
0	25.2	42.9	26.4	5.5
0.20	28.4	37.9	21.5	12.3
0.50	26.2	39.7	18.8	15.3
0.85	27.1	38.1	4.5	30.2

The crystal parameters of calcium aluminate compounds in clinkers with different P additions were calculated and listed in Table 2. $C_{12}A_7$ belongs to the cubic system with $I\bar{4}3d$ space group, and CA belongs to the monoclinic system with $P21/n$ space group. As the P addition increases, the lattice constant (a) of $C_{12}A_7$ decreases gradually, and the corresponding cell volume (V) decreases. Meanwhile, the lattice constant a of CA decreases while the b and c increase with increasing P addition, and the corresponding cell volume increases gradually. Because no P-containing phase was found in the XRD patterns, the changes in the lattice constants and cell volumes of $C_{12}A_7$ and CA indicate that P can form solid solutions in calcium aluminates, which is also proved by the following P distribution in the calcium aluminate clinker according to the map scan analysis of SEM.

Table 2 Crystal parameters of calcium aluminates in clinkers with different P additions

P addition/wt.%	$C_{12}A_7$		CA			
	$a=b=c$/nm	V/nm^3	a/nm	b/nm	c/nm	V/nm^3
0	1.1997	1.7267	0.8689	0.8125	1.5037	1.0616
0.20	1.1988	1.7228	0.8679	0.8129	1.5090	1.0646
0.50	1.1982	1.7202	0.8654	0.8135	1.5172	1.0681
0.85	1.1980	1.7194	0.8651	0.8143	1.5319	1.0791

3.3 Morphology of calcium aluminate clinker

The SEM image of clinker sintered with 0.85% P is shown in Fig. 3. The morphology of clinker is divided to three regions, i.e. light grey, medium grey and dark gray, which are adjacent to each other but the borderlines are clearly discerned. The micro-compositions of the three regions determined by EDS are listed in Table 3, and the corresponding C/A ratio (the molar ratio of CaO to Al_2O_3) and C/S ratio (the molar ratio of CaO to SiO_2) were calculated.

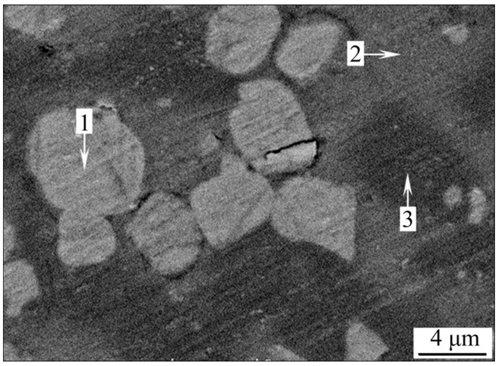

Fig. 3 SEM image of calcium aluminate clinker containing 0.85% P

Table 3 EDS results of clinker corresponding to Fig. 3 (at.%)

Point No.	Ca	Al	Si	C/A	C/S
1	34.39	−	15.95	−	2.16
2	21.25	27.26	−	1.56	−
3	15.70	34.38	−	0.91	−

The light grey region (Point 1 in Fig. 3) is mainly composed of Ca, Si and O, and the C/S ratio is about 2, which corresponds to C_2S based on the XRD results. The crystal size of C_2S is 2−8 μm. Both the medium grey region (Point 2) and the dark gray region (Point 3) are composed of Ca, Al and O, but the C/A ratios are quite different. According to the C/A ratios and XRD results, the medium grey region corresponds to $C_{12}A_7$, while the the dark gray region corresponds to CA.

The elemental distribution of calcium aluminate clinker when sintered with 0.85% P was obtained by map scan analysis of SEM, as shown in Fig. 4. The elements of Ca, O and P distribute evenly, while Al mostly distributes in the medium grey and dark gray regions where the calcium aluminate compounds distribute. Si mainly distributes in the light gray region of C_2S.

3.4 Thermal analysis

The DSC and TG curves of the mixtures of $CaCO_3$, Al_2O_3 and SiO_2 without P and with 0.85% P during heating process are shown in Fig. 5. The mass of both TG curves has little change over 800 °C after the decomposition of $CaCO_3$, but a series of endothermic peaks appear in the DSC curves. According to the related references [8,9], the endothermic peaks at 1100−1300 °C represent the reactions of C_2S formation. As CA is the main calcium aluminate compound in the clinkers, the endothermic peaks at 1334.8 °C in Fig. 5(a) and at 1331.0 °C in Fig. 5(b) are related to the formation of CA, while the endothermic peaks at 1382.9 °C in Fig. 5(a) and at 1374.3 °C in Fig. 5(b) are related to the formation of $C_{12}A_7$. The P addition decreases the formation temperatures of calcium aluminate compounds in clinkers, which has the same effect with Na_2O [16].

Combining the macrostructure and the XRD analyses of the clinkers with the DSC results, the following conclusions can be drawn: P can decrease the mineral formation temperature and the melting temperature of clinkers, and distributes evenly in the liquid which forms solid solutions in both calcium

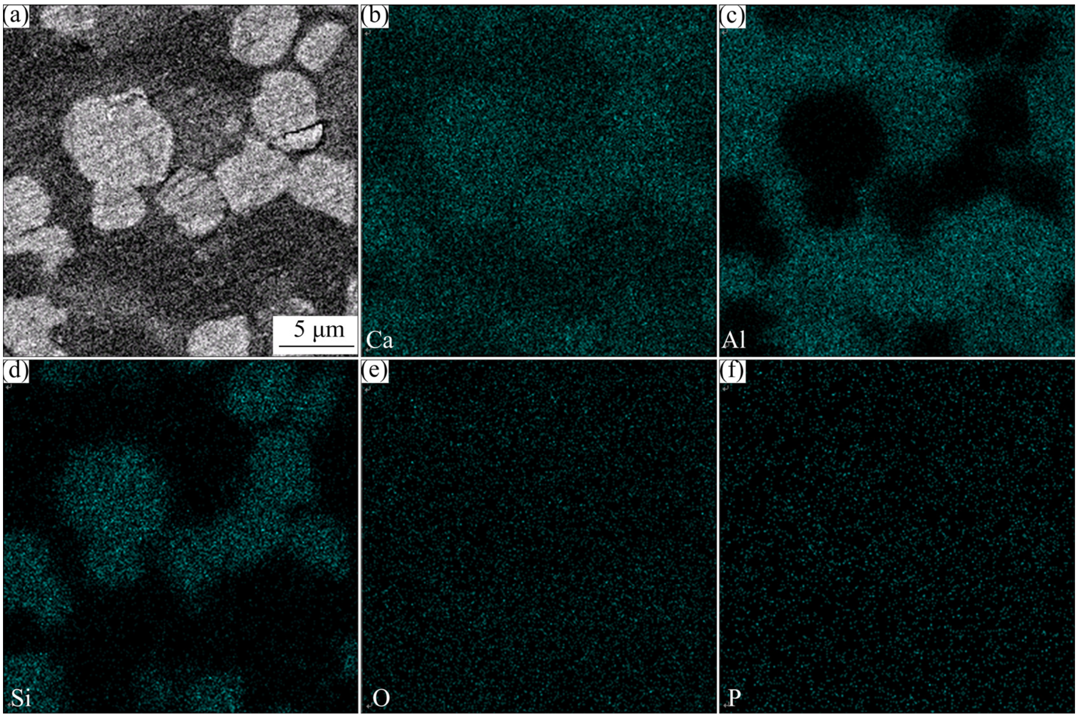

Fig. 4 SEM image (a) and elemental distributions (b−f) of calcium aluminate clinker containing 0.85% P

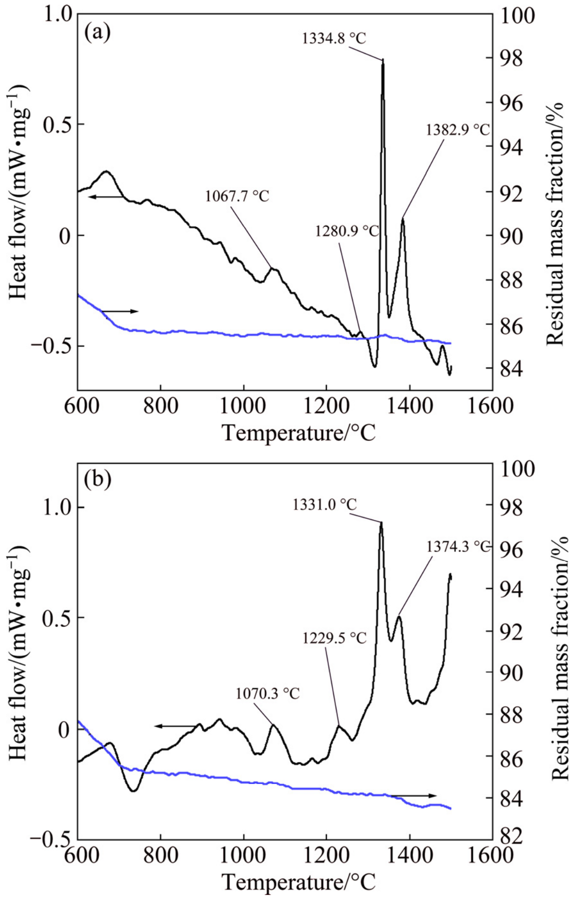

Fig. 5 DSC−TG curves of mixtures without P (a) and with 0.85% P (b) during heating process

aluminates and dicalcium silicate; then P inhibits the transformation of β-C_2S to γ-C_2S, which makes the clinkers glassy and unpulverized.

3.5 Leaching property of calcium aluminate clinkers

The leaching reactions of calcium aluminate compounds in sodium carbonate solution are shown in Formulae (4) and (5), respectively. Meanwhile, C_2S can also react with the alkali solution as listed in Formulae (6) and (7), and then transform to the corresponding desilication products (DSPs) as listed in Formulae (8) and (9) known as the secondary reaction in the sinter process [23]. The leaching results of clinkers with different P additions in sodium carbonate solution are shown in Table 4. The concentrations of caustic alkali and alumina in sodium aluminate solution after leaching decrease with increasing P addition, especially an obvious decrease when the P addition reaches 0.85%.

The Al_2O_3 leaching rate of clinkers and the molar ratio of caustic alkali to alumina (α_K) in sodium aluminate solution after leaching were calculated and shown in Fig. 6. Both the Al_2O_3 leaching rate and α_K decrease with increasing P addition. The Al_2O_3 leaching rate decreases from 95.01% to 90.26% when the P addition increases from 0 to 0.50%; as the P addition increases to 0.85%, the Al_2O_3 leaching rate is only 83.34%, demonstrating that P deteriorates the leaching properties of clinkers.

$$\begin{aligned}&12CaO\cdot 7Al_2O_3(s)+12Na_2CO_3(l)+33H_2O{=\!=}\\&\quad 12CaCO_3(s)+14NaAl(OH)_4(l)+10NaOH(l)\end{aligned} \tag{4}$$

$$\begin{aligned}&CaO\cdot Al_2O_3(s)+Na_2CO_3(l)+4H_2O{=\!=}\\&\quad CaCO_3(s)+2NaAl(OH)_4(l)\end{aligned} \tag{5}$$

$$\begin{aligned}&2CaO\cdot SiO_2(s)+2NaOH(l)+H_2O{=\!=}\\&\quad 2Ca(OH)_2(l)+Na_2SiO_3(l)\end{aligned} \tag{6}$$

$$\begin{aligned}&2CaO\cdot SiO_2(s)+2Na_2CO_3(l)+H_2O{=\!=}\\&\quad 2CaCO_3(s)+Na_2SiO_3(l)+2NaOH(l)\end{aligned} \tag{7}$$

$$\begin{aligned}&1.7Na_2SiO_3(l)+2NaAl(OH)_4(l){=\!=}\\&\quad Na_2O\cdot Al_2O_3\cdot 1.7SiO_2\cdot nH_2O(s)+\\&\quad 3.4NaOH(l)+(2.3-n)H_2O\end{aligned} \tag{8}$$

$$\begin{aligned}&3Ca(OH)_2(l)+xNa_2SiO_3(l)+2NaAl(OH)_4(l){=\!=}\\&\quad 3CaO\cdot Al_2O_3\cdot xSiO_2\cdot(6-2x)H_2O(s)+\\&\quad 2(x+1)NaOH(l)+xH_2O\end{aligned} \tag{9}$$

Table 4 Leaching results of calcium aluminate clinkers with different P additions

P addition/ wt.%	Liquor concentration/ ($g\cdot L^{-1}$)			Solid composition/wt.%	
	N_K	N_T	AO	Al_2O_3	SiO_2
0	30.75	78.66	38.81	1.64	8.22
0.20	30.25	80.22	38.26	2.15	9.14
0.40	29.25	80.66	37.57	3.03	10.46
0.50	27.93	80.45	36.53	4.11	10.55
0.85	25.73	78.81	34.75	5.84	9.04

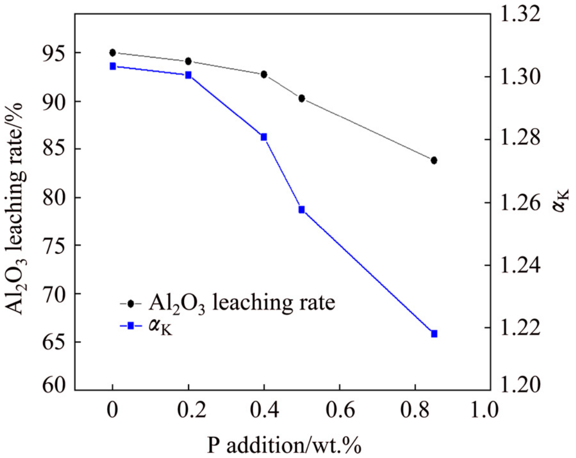

Fig. 6 Al_2O_3 leaching rate and α_K of calcium aluminate clinkers with different P additions after leaching

The XRD patterns of the leached residues without P and with 0.85% P are shown in Fig. 7. The main minerals in the leached residues are $CaCO_3$, β-C_2S and γ-C_2S because of the decomposition of calcium aluminate compounds. However, some $C_{12}A_7$ still exists in the residue when the clinker contains P impurity, demonstrating that P deteriorates the leaching activity of $C_{12}A_7$ of clinkers in sodium carbonate solution. In addition, CA is not found in both residues with and without P addition, indicating that the leaching property of CA is good and it is not affected by the P impurity.

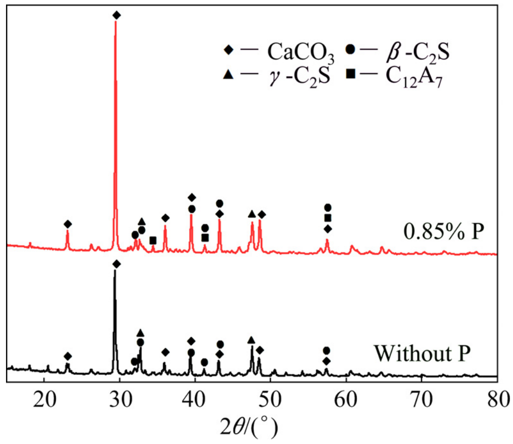

Fig. 7 XRD patterns of leached residues of calcium aluminate clinkers without P and with 0.85% P

No DSPs were found in the leached residues, as seen in Fig. 7, indicating that the secondary reaction of C_2S does not happen because of the high liquid-to-solid ratio during leaching [23,24]. As listed in Formulae (4) and (5), the decomposition of $C_{12}A_7$ in sodium carbonate solution leads to the increase of N_K because of the extra formation of NaOH as compared to CA. On the other hand, as shown in Table 1, the addition of P during sintering can increase the content of $C_{12}A_7$ but decrease the content of CA. However, the N_K in sodium aluminate solution after leaching decreases with the increase of P addition as seen in Fig. 6, which also demonstrates that P increases the stability of $C_{12}A_7$ during the sintering process and then results in more un-decomposed $C_{12}A_7$ in clinker during leaching.

Therefore, P has a negative impact on the sintering and leaching properties of calcium aluminate clinkers in $CaO-Al_2O_3-SiO_2$ system. P cannot only inhibit the transformation of β-C_2S to γ-C_2S to deteriorate the self-pulverization property of clinker, but also form solid solutions in calcium aluminates to decrease the alumina leaching rate of clinker. The content of P should be controlled to be less than 0.50% in the final calcium aluminate clinker.

4 Conclusions

(1) The self-pulverization properties of calcium aluminate clinkers are increasingly deteriorated by increasing P addition because P hinders the transformation of β-C_2S to γ-C_2S.

(2) The clinkers mainly contains $C_{12}A_7$, CA, β-C_2S and γ-C_2S, but the content of β-C_2S increases while the content of γ-C_2S decreases as the P addition increases.

(3) The cell volumes of $C_{12}A_7$ and CA decrease and increase respectively as the P addition increases, and P decreases the formation temperatures of calcium aluminates and increases the stability of $C_{12}A_7$ during sintering.

(4) The Al_2O_3 leaching rate of calcium aluminate clinkers decreases from 95.01% to 83.84% as the P addition increases from 0 to 0.85%. The content of P should be controlled to be less than 0.50% in the calcium aluminate clinker.

References

[1] AKONO A, CUI Y, KATARUKA A, ANDERSON K, KABIR P. Intrinsic mechanical properties of calcium aluminate crystals via the linear comparison composite method coupled with nano-indentation [J]. Mechanics of Materials, 2018, 118: 74−84.

[2] LEE N K, KOH K T, PARK S H, RYU G S. Microstructural investigation of calcium aluminate cement-based ultra-high performance concrete (UHPC) exposed to high temperatures [J]. Cement and Concrete Research, 2017, 102: 109−118.

[3] YANG Shou-lei, XIAO Guo-qing, DING Dong-hai, REN Yun, LV Li-hua, YANG Pan. Dissolution−precipitation mechanism of combustion synthesis of calcium aluminate [J]. Ceramics International, 2017, 43(17): 15918−15926.

[4] KANG Shuai, WANG Xue, XU Wen-bin, WANG Xin, HE Dong-bing, HU Li-li. Effect of B_2O_3 content on structure and spectroscopic properties of neodymium-doped calcium aluminate glasses [J]. Optical Materials, 2017, 66: 287−292.

[5] FABRICHNAYA O B, NERÁD I. Thermodynamic properties of liquid phase in the $CaO\cdot SiO_2-CaO\cdot Al_2O_3\cdot 2SiO_2-2CaO\cdot Al_2O_3\cdot SiO_2$ system [J]. Journal of the European Ceramic Society, 2000, 20(4): 505−515.

[6] RODRÍGUEZ M A, AGUILAR C L, AGHAYAN M A. Solution combustion synthesis and sintering behavior of $CaAl_2O_4$ [J]. Ceramics International, 2012, 38(1): 395−399.

[7] CHEN Guo-hua. Mechanical activation of calcium aluminate formation from $CaCO_3-Al_2O_3$ mixtures [J]. Journal of Alloys and Compounds, 2006, 416(1−2): 279−283.

[8] MOHAMED B M, SHARP J H. Kinetics and mechanism of formation of monocalcium aluminate, $CaAl_2O_4$ [J]. Journal of Materials Chemistry, 1997, 7(8): 1595−1599.

[9] MOHAMED B M, SHARP J H. Kinetics and mechanism of formation of tricalcium aluminate, $Ca_3Al_2O_6$ [J]. Thermochimica Acta, 2002, 388(1−2): 105−114.

[10] OSTROWSKI C, ELAZNY J. Solid solutions of calcium aluminates C_3A, $C_{12}A_7$ and CA with sodium oxide [J]. Journal of Thermal Analysis and Calorimetry, 2004, 75(3): 867−885.

[11] STÖBER R, NOFZ M, GEBNER W, SCHRÖTER C, KRANZ G. Paramagnetic monitors (Mn^{2+}, Mn^{4+}, Fe^{3+}, and O^{2-}) in the solid-state reaction yielding $12CaO\cdot 7Al_2O_3$ and other aluminates [J]. Journal of Solid State Chemistry, 1989, 81(2): 152−164.

[12] VERMA R K, KAUR G, RAI A, RAI S B. Dual mode green fluorescence from Tb^{3+}: $Ca_{12}Al_{14}O_{33}$ and its applicability as delayed fluorescence [J]. Materials Research Bulletin, 2012, 47(11): 3726−3731.

[13] CHOU K S, BURNET G. Formation of calcium aluminates in the

lime-sinter process [J]. Cement and Concrete Research, 1981, 11(2): 167−174.

[14] TIAN Yong-pan, PAN Xiao-lin, YU Hai-yan, TU Gan-feng. Formation mechanism of calcium aluminate compounds based on high-temperature solid-state reaction [J]. Journal of Alloys and Compounds, 2016, 670: 96−104.

[15] ZHANG Di, PAN Xiao-lin, YU Hai-yan, ZHAI Yu-chun. Mineral transition of calcium aluminate clinker during high-temperature sintering with low lime dosage [J]. Journal of Materials Science and Technology, 2015, 31(12): 1244−1250.

[16] YU Hai-yan, PAN Xiao-lin, WANG Bo, ZHANG Wu, SUN Hui-lan, BI Shi-wen. Effect of Na_2O on the formation of calcium aluminates in the $CaO-Al_2O_3-SiO_2$ system [J]. Transactions of Nonferrous Metals Society of China, 2012, 22(12): 3108−3112.

[17] YU Hai-yan, PAN Xiao-lin, LIU Bao-wei, WANG Bo, BI Shi-wen. Effect of iron oxides on the activity of calcium aluminate clinker in $CaO-Al_2O_3-SiO_2$ system [J]. Journal of Iron and Steel Research, International, 2014, 21(11): 990−994.

[18] WANG Bo, SUN Hui-lan, GUO Dong, ZHANG Xue-zheng. Effect of Na_2O on alumina leaching property and phase transformation of MgO-containing calcium aluminate slags [J]. Transactions of Nonferrous Metals Society of China, 2011, 21(12): 2752−2757.

[19] WANG Bo, CHU Wei-qin, HAO Yuan-liang, RONG Shuo, SUN Hui-lan. Synthesis and alumina leaching mechanism of calcium sulphoaluminate [J]. Transactions of Nonferrous Metals Society of China, 2017, 27(9): 2090−2095.

[20] PAN Xiao-lin, YU Hai-yan, TU Gan-feng. Reduction of alkalinity in bauxite residue during Bayer digestion in high-ferrite diasporic bauxite [J]. Hydrometallurgy, 2015, 151: 98−106.

[21] GHOSH S N, RAO P B, PAUL A K, RAINA K. The chemistry of dicalcium silicate mineral [J]. Journal of Materials Science, 1979, 14(7): 1554−1566.

[22] ÁNGELES G, KHADIJA M, MOHAMMED Z, ARANDA A G. In situ synchrotron powder diffraction study of active belite clinkers [J]. Journal of Applied Crystallography, 2007, 40(6): 999−1007.

[23] YU Hai-yan, WANG Bo, PAN Xiao-lin, Ding Ting-ting, BI Shi-wen. Electrochemical study on adsorption behavior of surfactants at β-$2CaO\cdot SiO_2/NaAlO_2$ interface [J]. Transactions of Nonferrous Metals Society of China, 2013, 23(8): 2416−2421.

[24] SUN Hui-lan, WANG Bo, ZHANG Jian-xin, ZONG Shu-feng, LIU Jia-jia. Secondary reaction mechanism of leaching process of calcium aluminate slag [J]. Transactions of Nonferrous Metals Society of China, 2015, 25(4): 1334−1340.

P 含量对 $CaO-Al_2O_3-SiO_2$ 体系在高温烧结过程中矿相转变的影响

于海燕，潘晓林，董凯伟，吴 艳

东北大学 冶金学院，沈阳 110819

摘 要：采用 XRF、XRD、SEM−EDS 和 DSC−TG 等技术手段研究不同 P 含量下铝酸钙熟料在高温烧结过程中的矿相转变、显微组织、自粉性能及其氧化铝浸出性能。1350 °C 下烧结熟料主要由 $12CaO\cdot 7Al_2O_3$、 $CaO\cdot Al_2O_3$、β-$2CaO\cdot SiO_2$ 和 γ-$2CaO\cdot SiO_2$ 等矿相组成；随着 P 含量的增加，β-$2CaO\cdot SiO_2$ 含量逐渐升高，而 γ-$2CaO\cdot SiO_2$ 含量逐渐降低。熟料的自粉性能随着 P 含量的增加逐渐恶化。P 在熟料中均匀分布，其存在抑制 β-$2CaO\cdot SiO_2$ 向 γ-$2CaO\cdot SiO_2$ 的转变。$12CaO\cdot 7Al_2O_3$ 和 $CaO\cdot Al_2O_3$ 的晶胞体积随着 P 含量的增加分别降低和提高，且 P 能降低铝酸钙化合物的形成温度。铝酸钙熟料的氧化铝浸出率随着 P 含量的增加明显降低，当 P 含量从 0 提高到 0.85%时，氧化铝浸出率从 95.01%降低到 83.84%。

关键词：石灰烧结法；铝酸钙；硅酸二钙；晶体结构；自粉性能；浸出

(Edited by Wei-ping CHEN)